

# Nonreciprocal optical solitons against backscattering

BAIJUN LI<sup>1</sup>, ŞAHİN. K. ÖZDEMİR<sup>2</sup>, LIN ZHANG<sup>3</sup>, AND HUI JING<sup>1,\*</sup>

<sup>1</sup>Key Laboratory of Low-Dimensional Quantum Structures and Quantum Control of Ministry of Education, Department of Physics and Synergetic Innovation Center for Quantum Effects and Applications, Hunan Normal University, Changsha 410081, China

<sup>2</sup>Department of Engineering Science and Mechanics, and Materials Research Institute, Pennsylvania State University, University Park, State College, Pennsylvania 16802, USA

<sup>3</sup>School of Physics and Information Technology, Shaanxi Normal University, Xi'an 710061, China

\*Corresponding author: jinghui73@foxmail.com

Compiled December 22, 2024

We propose how to create and manipulate nonreciprocal solitons in a rotation-managed optical Kerr resonator and maintain its quality against backscattering losses. We show that by spinning the resonator, optical solitons with different numbers can appear in different directions due to the Sagnac-Fizeau drag effect. Therefore, unidirectional solitons can be observed by driving the resonator from one side but not the other. In particular, we find that these nonreciprocal solitons are more robust against backscattering losses by controlling the rotation speed of the resonator. Our work, bridging the fields of nonreciprocal physics and soliton science, represents a new stable nonreciprocal device and a promising technique for one-way soliton isolators or lasers, backaction-immune soliton communications, and enhanced soliton-comb metrology. © 2024 Optical Society of America

<http://dx.doi.org/10.1364/ao.XX.XXXXXX>

Solitons or robust waveforms preserving shape or energy in propagation, widely exist in natural and artificial systems [1–6], and are indispensable in diverse applications such as telecommunication, microwave generation, and metrology. In recent years, rapid advances have been witnessed in manipulating and utilizing dissipative Kerr solitons created in microresonators, featuring balances of the dispersion and nonlinearity, as well as the loss and gain [7–12]. Optical dissipative Kerr solitons have become a unique platform for compact and low power frequency-comb generation, with femtosecond optical pulses at tens of gigahertz repetition rates [13–15], enabling disruptive technologies such as chip-scale clocks, integrated optical frequency synthesizer [16], and ultrafast ranging [17–19].

Here we propose how to achieve nonreciprocal dissipative Kerr solitons which enable various one-way devices such as pulse router [20] or chiral combs [21]. We note that the nonreciprocal devices, allowing one-way flow of information and thus playing key roles in backaction-immune communications or invisible sensings, have been achieved in nonlinear systems [22–31], temporal devices [32–34], non-Hermitian systems [35–37], and spinning resonators or single-photon devices [38–41]. By steering the freedom of rotation, novel effects have also been

shown such as sound circulation [42], unidirectional phonon laser [43] and nonreciprocal entanglement [44], as well as ultrasensitive sensing [45, 46] and anti-parity-time symmetry device [47]. However, manipulating solitons in a nonreciprocal way and achieving robust solitons against backscattering losses by means of a spinning microresonator, to our knowledge, have not been studied previously.

In this letter, we find the dissipative Kerr solitons with different numbers can emerge in different directions by spinning a Kerr resonator. One-way solitons can be observed when the resonator is driven in one direction but not the other. Specifically, we find these nonreciprocal solitons are more robust against backscattering losses by controlling the rotation speed of the resonator. These results, building a bridge between such two active fields as nonreciprocal physics and soliton science, provide a novel strategy to achieve one-way solitons, which has wide applications in soliton isolators or lasers [48], backaction-immune soliton communications [2, 49], and soliton metrology [50, 51].

To set the stage, we consider a spinning Kerr microresonator, driven by a Gaussian pulse with frequency  $\omega_d$  from the left or right side via the evanescent field of a nearby tapered fiber [52] (see Fig. 1). The clockwise (CW) and counter-clockwise (CCW) modes of the resonator are coupled to each other via the backscattering process due to inhomogeneous materials or random defects. In a very recent experiment, by using a spinning microresonator with the radius  $r = 1.1\text{mm}$  and the maximal rotation frequency  $\Omega = 6.6\text{ kHz}$  [38], 99.6% optical isolation was achieved for an input signal. In such a device, the frequency of incident laser changes slightly when light enters the spinning resonator, i.e.,  $\omega_{\pm} - \omega = \pm \frac{\Omega R n}{c} \omega$ , where the subscript  $\pm$  denotes the light propagating against or along the spinning direction,  $c$  is the speed of light in the vacuum, and  $n$  or  $R$  is the refractive index or the radius of the cavity. Since  $n(\omega_{\pm}) \approx n(\omega) + (\omega_{\pm} - \omega) \frac{dn(\omega)}{d\omega}$ , in view of the Lorentz transformation, we have the speed of light in the spinning resonator as

$$\mathbf{v}_{\pm} = \frac{u_{\pm} \pm \Omega R}{1 \pm \Omega R u_{\pm} / c^2}, \quad (1)$$

with

$$u_{\pm} = \frac{c}{n(\omega_{\pm})} \approx \frac{c}{n} \mp \frac{\omega}{n} \frac{dn}{d\omega} \Omega R. \quad (2)$$

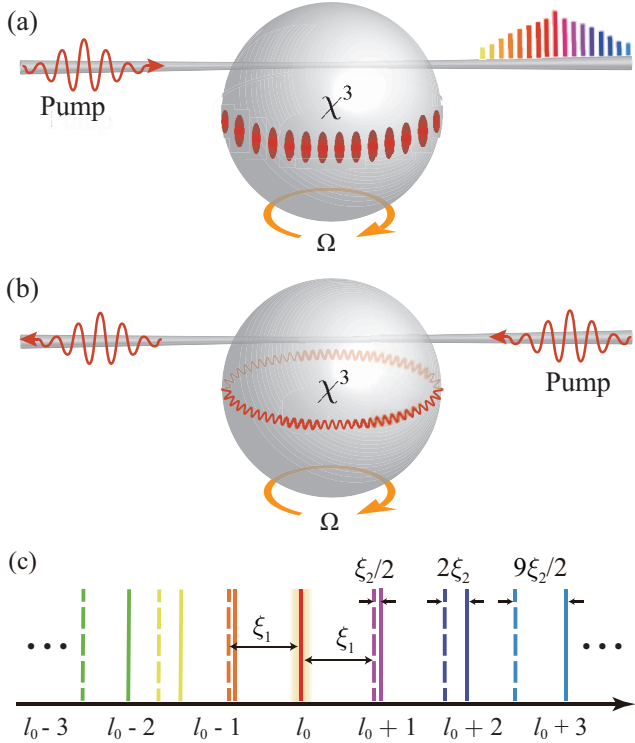


**Fig. 1. Schematic illustration of nonreciprocal solitons.** By spinning the Kerr microresonator, different Sagnac frequency shifts,  $\Delta_F$ , can be induced for counter-circulating modes. (a-b) When an input laser coming from the one side, solitons can appear, while disappearing from the other side. (c) Eigenmodes of microresonator with anomalous dispersion. The solid lines indicate the real position of the eigenfrequencies, while the dashed lines represent the location if the dispersion were null. Here the higher-order dispersions ( $\xi_3, \xi_4, \dots$ ) have been ignored.

The optical frequencies of the counter-propagating lights are then

$$\nu_{\pm} = \frac{\beta \mathbf{v}_{\pm}}{2\pi R} \approx \frac{\beta}{2\pi R} \left[ \frac{c}{n} \pm \Omega R \left( 1 - \frac{1}{n^2} - \frac{\omega}{n} \frac{dn}{d\omega} \right) \right], \quad (3)$$

with  $\beta = 1, 2, 3, \dots$ , leading to the Sagnac shifts [38, 53], i.e.,  $\omega_0 \rightarrow \omega_0 \pm \Delta_F$ ,

$$\pm \Delta_F = 2\pi(\nu_{\pm} - \nu_0) = \pm \omega_0 \frac{n\Omega R}{c} \left( 1 - \frac{1}{n^2} - \frac{\lambda}{n} \frac{dn}{d\lambda} \right), \quad (4)$$

where  $\nu_0 = \frac{\beta c}{2\pi n R}$ , and  $\omega_0 = 2\pi c/\lambda$  is the pump frequency for the static resonator. The dispersion term  $dn/d\lambda$ , characterizing the relativistic origin of the Sagnac effect, is relatively small in typical materials ( $\sim 1\%$ ) [38, 53]. The light drag can be further enhanced by dispersions, as demonstrated also in an experiment using a moving microcavity [54]. Here, for convenience, we consider only the CW rotation of the microresonator. Also we focus on the fundamental modes denoted by an integer wave number  $l$  (around the eigen-number  $l_0$  of the pump), the eigenfrequencies of which can be expanded as [7]

$$\omega_l = \omega_0 + \sum_{n=1}^N \frac{\xi_n}{n!} (l - l_0)^n, \quad (5)$$

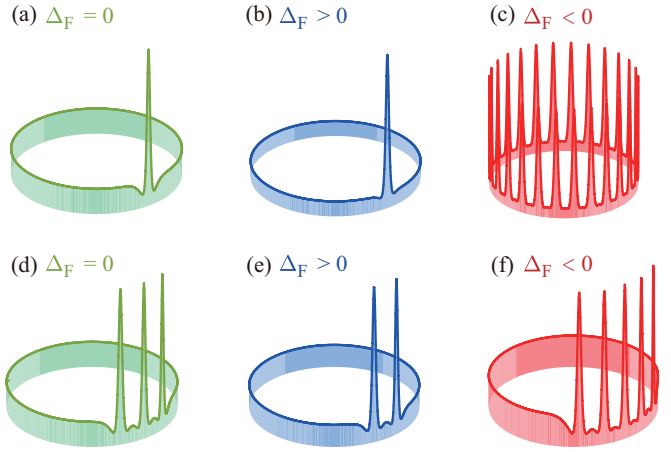


**Fig. 2. Optical solitons with different numbers in different directions.** The three-dimensional representations of transient dynamics  $|\psi|^2$  at  $\tau = 200$  in a static cavity and spinning Kerr resonator. The initial conditions are Gaussian pulses: (a-c)  $\psi_0 = 0.5 + \exp[-(\theta/0.1)^2]$ , (d-f)  $\psi_0 = 0.5 + \exp[-(\theta/0.55)^2]$ , the rotation velocity (a-c)  $\Omega = 2.0$  kHz, (d-f)  $\Omega = 350$  Hz. The other parameters are  $\beta = -0.004$ ,  $F = 1.37$ ,  $\Delta_p = 2$ , and we do not display the  $xyz$  coordinate axis for convenience since the numbers of solitons can be seen from the waveform.

where  $\xi_1 = d\omega/dl|_{l=l_0} = c/(nr)$  is the free spectral range, and  $\xi_2 = d^2\omega/dl^2|_{l=l_0}$  is the second-order dispersion coefficient, leading to asymmetric eigenfrequencies [see Fig. 1(c)].

The dynamics of this system can be described by the spatiotemporal Lugiato-Lefever equation (LLE) [55–58]

$$\frac{\partial \psi}{\partial \tau} = -[1 + i(\Delta_p - \Delta_{\text{sag}})]\psi + i|\psi|^2\psi - i\frac{\beta}{2}\frac{\partial^2 \psi}{\partial \theta^2} + iJ\phi + F, \quad (6)$$

$$\frac{\partial \phi}{\partial \tau} = -[1 + i(\Delta_p + \Delta_{\text{sag}})]\phi + i|\phi|^2\phi - i\frac{\beta}{2}\frac{\partial^2 \phi}{\partial \theta^2} + iJ\psi, \quad (7)$$

where  $\psi$  and  $\phi$  denote the slowly varying field envelope of the optical modes. The backscattering process, as observed in experiments [59–62], is denoted by the strength  $J_0$ ;  $\theta \in [-\pi, \pi]$  is the azimuthal angle along the circumference of the resonator;  $\tau = kt/2$  is the dimensionless time; the other scaled parameters are  $J = -2J_0/\kappa$ ,  $\Delta_p = -2\delta/\kappa$ ,  $\beta = -2\xi_2/\kappa$ ,  $\Delta_{\text{sag}} = 2\Delta_F/\kappa$ , with  $\kappa = \omega_0/Q$  is the optical loss rate with the cavity quality factor  $Q$ , and  $\delta = \omega_d - \omega_0$  is the detuning between the pump and the cavity resonance. Also,  $F = \sqrt{4gP/(\kappa^2 \hbar \omega_d)}$  denotes the pump field intensity, with the laser power  $P$  and the optical gain  $g = n_2 c \hbar \omega_d^2 / n^2 V_0$ , where  $n$  or  $n_2$  is the linear or nonlinear refraction indice of the bulk material, respectively, and  $V_0$  is the effective volume of the microresonator.

We first consider the case without any backscattering. We choose experimentally feasible parameter values [63], i.e., the optical wavelength  $\lambda = 1550$  nm,  $Q = 10^9$ ,  $r = 30$   $\mu\text{m}$ ,  $\beta = -0.004$ ,  $n = 1.44$ , and  $\Omega = 2.2$  kHz. For a static resonator, we find that, as studied previously, optical solitons with different numbers appear under different pulses in a reciprocal way, i.e., regardless of the input direction [see Fig. 2(a-d)] [64]. In contrast, for a spinning device, the system exhibits giant nonreciprocity. Turing patterns emerge when driving the device on

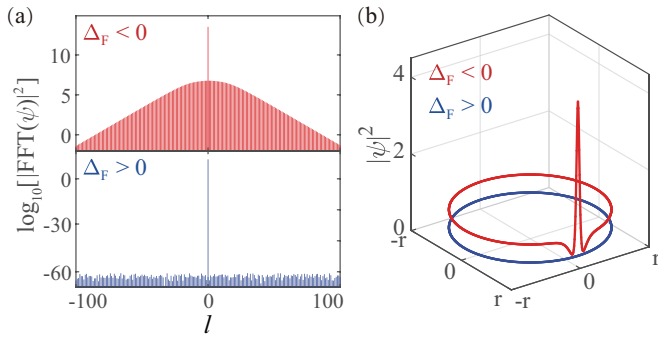


**Fig. 3. Nonreciprocal solitons.** Kerr combs and three-dimensional representations of transient dynamics at  $\tau = 200$  in a spinning Kerr microresonator. When the resonator is driven from the left-hand side, a single soliton can appear, while disappearing for the same input laser coming on the right-hand side. The detuning  $\Delta_p = 2.3$ , the rotation velocity  $\Omega = 2.2$  kHz, and the initial condition is a Gaussian pulse:  $\psi_0 = 0.5 + \exp[-(\theta/0.1)^2]$ . The other parameters are same as Fig. 2.

left-side side, while the same pulse is input from the opposite side the single soliton state appears. Interestingly, we find that in such a device, it is possible to realize directional switch of soliton numbers for multiple soliton pulses, which is otherwise challenging to be achieved in conventional devices [65, 66]. For an example, a three-soliton state can appear in a nonspinning resonator [64], while in a spinning device (with  $\Omega = 350$  Hz), a two-soliton or five-soliton state appears when the same pulse is input from the left side (blue curves) or the right side (red curves), as shown in Fig. 2(d-f). This unidirectional control of solitons can be used to make, e.g., soliton diode or circulator and nonreciprocal soliton laser or switch [20, 21, 48], for a wide range of practical applications in one-way soliton engineering or soliton-based communications [2, 49].

Clear signatures of nonreciprocal solitons can also be observed in Fig. 3. We find that soliton diodes can appear in this system, by tuning the parameter values. Setting  $\Delta_p = 2.3$  and  $\Omega = 2.2$  kHz, soliton only emerges when driving the device on left-side side, but is blocked when driving on the other side [see Fig. 3(b)]. This can be explained by the different Sagnac drag  $\Delta_F$  for the counter-circulating modes of the microresonator, with which the double balance (nonlinearity and anomalous dispersion, as well as gain and dissipation) becomes impossible to be maintained simultaneously for these two distinct modes. The possibility of achieving nonreciprocal solitons in an optical resonator, as far as we know, has not been revealed previously.

Nonreciprocal solitons also provide an unexpected way to protect optical devices against backscattering losses, without using specially constructed topological systems or a chiral environment [67, 68]. As Fig. 4 shows, for increased values of backscattering  $J$ , solitons tend to be unstable in a conventional static resonator, characterized by the emergence of random peaks. In contrast, for a spinning device, solitons can be more robust against backscattering losses. Figure 4(c-f) shows that, by choosing a suitable spinning velocity, i.e.,  $\Omega = 60$  kHz, the soliton shape can be even as that in an ideal device (without any backscattering process). This provides a conceptually new and practically feasible strategy to improve the performance of soliton devices by harnessing the power of nonreciprocity, which

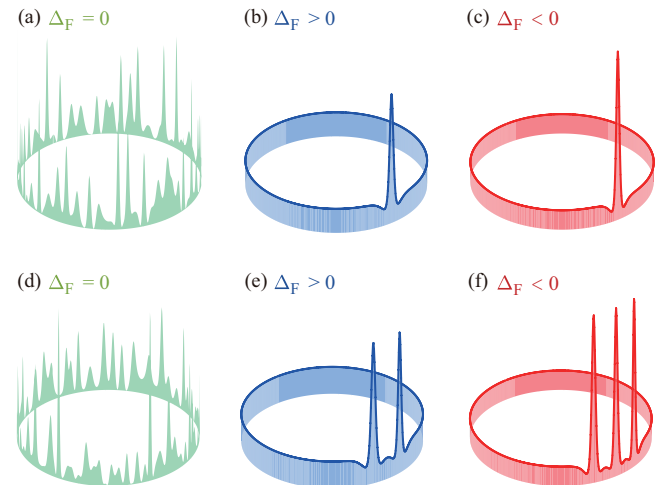


**Fig. 4. Suppression of soliton due to random-defect-induced backscattering, and its revival resulting from the rotation-induced compensation.** Three-dimensional representations of the transient dynamics  $|\psi|^2$  of CW mode at  $\tau = 200$  in a static and spinning microresonator when backscattering ( $J = 1$ ) is considered. The initial condition is a Gaussian pulse: (a-c)  $\psi_0 = 0.5 + \exp[-(\theta/0.1)^2]$ , (d-f)  $\psi_0 = 0.5 + \exp[-(\theta/0.55)^2]$ , the rotation velocity  $\Omega = 60$  kHz, and the detuning (a d)  $\Delta_p = 2.0$ , (b)  $\Delta_p = -6.9$ , (e)  $\Delta_p = -6.91$ , (c f)  $\Delta_p = 11$ . The other parameters are same as Fig. 2.

are crucial elements in optical communications [2, 49] and high-precision metrology [50, 51].

In summary, we have proposed how to engineer optical solitons in a highly nonreciprocal way. We find that by spinning an optical Kerr resonator and then driving it on different sides, optical solitons with different numbers can be observed in such a device. These nonreciprocal solitons are robust against backscattering losses which are otherwise detrimental for conventional devices. We expect that nonreciprocal solitons are achievable in systems well beyond spinning photonics, such as the existing nonreciprocal techniques using solid devices [22, 23], atoms [26, 27], or synthetic materials [34–37]. In a broader view, our work builds a bridge between nonreciprocal physics and soliton science, providing new ways to achieve e.g., backaction-immune soliton communications [2, 49] or enhanced soliton metrology [50, 51].

**Funding.** We thank Zheng Yu Wang, HuiLai Zhang, and Prof. FangJie Shu for helpful discussions. HJ is supported by the National Science Foundation of China (NSFC, 11474087 and 11774086, 11935006). LZ is supported by the National Natural Science Foundation of China for emergency management project (Grant No.11447025).

**Note added.** After finishing this work, we noticed a paper also revealing the possibility of achieving one-way soliton in a single resonator, but using cross-kerr nonlinearity and dual optical pump [69].

**Disclosures.** The authors declare no conflicts of interest.

## REFERENCES

1. A. Hasegawa and Y. Kodama, *Solitons in Optical Communications* (Oxford: Oxford University Press) (1995).
2. H. A. Haus, W. S. Wong, "Solitons in optical communications," *Reviews of Modern Physics* **68**(2), 423–444 (1996).

3. N. J. Zabusky, M. D. Kruskal, "Interaction of "solitons" in a collisionless plasma and the recurrence of initial states," *Phys. Rev. Lett.* **15**, 240–243 (1965).

4. L. F. Mollenauer, R. H. Stolen, J. P. Gordon, "Experimental observation of picosecond pulse narrowing and solitons in optical fibers," *Phys. Rev. Lett.* **45**, 1095–1098 (1980).

5. K. E. Strecker, G. B. Partridge, A. G. Truscott, R. G. Hulet, "Formation and propagation of matterwave soliton trains," *Nature* **417**, 150–153 (2002).

6. T. Ackemann, W. J. Firth, and G. Oppo, "Fundamentals and Applications of Spatial Dissipative Solitons in Photonic Devices," *Advances in Atomic Molecular and Optical Physics* 323–421 (2009).

7. T. Herr, V. Brasch, J. D. Jost, C. Y. Wang, N. M. Kondratić, M. L. Gorodetsky, and T. J. Kippenberg, "Temporal solitons in optical microresonators," *Nature Photon.* **8**(2), 145–152 (2014).

8. X. Yi, Q.-F. Yang, K. Y. Yang, M.-G. Suh, K. Vahala, "Soliton frequency comb at microwave rates in a high-Q silica microresonator," *Optica* **2**, 1078 (2015).

9. V. Brasch, M. Geiselmann, T. Herr, G. Lihachev, M. H. P. Pfeiffer, M. L. Gorodetsky, T. J. Kippenberg, "Photonic chip-based optical frequency comb using soliton Cherenkov radiation," *Science* **351**, 357–360 (2016).

10. R. Niu, S. Wan, S.-M. Sun, T.-G. Ma, H.-J. Chen, W.-Q. Wang, Z. Z. Lu, W.-F. Zhang, G.-C. Guo, C.-L. Zou, C.-H. Dong, "Repetition rate tuning of soliton in microrod resonators," *arXiv:1809.064490* (2018).

11. F. J. Shu, P. J. Zhang, Y. J. Qian, Z. Y. Wang, S. Wan, C. L. Zou, G. C. Guo, and C. H. Dong, "A mechanically tuned Kerr comb in a dispersion-engineered silica microbubble resonator," *SCIENCE CHINA Physics, Mechanics & Astronomy* **63**(5), 254211 (2020).

12. S. Wan, R. Niu, Z.-Y. Wang, J.-L. Peng, M. Li, G.-C. Guo, C.-L. Zou, and C.-H. Dong, "Frequency stabilization and tuning of breathing solitons in Si3N4 microresonators," *Photonics Research* **8**, 1342–1349 (2020).

13. T. J. Kippenberg, A. L. Gaeta, M. Lipson, and M. L. Gorodetsky, "Dissipative Kerr solitons in optical microresonators," *Science* **361**(6402), 129–162 (2018).

14. A. L. Gaeta, M. Lipson, and T. J. Kippenberg, "Photonic-chip-based frequency combs," *Nature Photonics* **13**, 158–169 (2019).

15. T. Fortier, and E. Baumann, "20 years of developments in optical frequency comb technology and applications," *Communications in Physics* **2**, 1–16 (2019).

16. D. T. Spencer, T. Drake, T. C. Briles, J. Stone, L. C. Sinclair, C. Fredrick, Q. Li, D. Westly, B. R. Ilic, A. Bluestone, N. Volet, T. Komljenovic, L. Chang, S. H. Lee, D. Yoon Oh, M.-G. Suh, K. Y. Yang, M. H. P. Pfeiffer, T. J. Kippenberg, E. Norberg, L. Theogarajan, K. Vahala, N. R. Newbury, K. Srinivasan, J. E. Bowers, S. A. Diddams, S. B. Papp, "An optical-frequency synthesizer using integrated photonics," *Nature* **557**, 81–85 (2018).

17. P. Trocha, M. Karpov, D. Ganin, M. H. Pfeiffer, A. Kordts, S. Wolf, J. Krockenberger, P. Marin-Palomo, C. Weimann, S. Randal, W. Freude, T. J. Kippenberg, C. Kooset, "Ultrafast optical ranging using microresonator soliton frequency combs," *Science* **359**(6378), 887–891 (2018).

18. M.-G. Suh and K. J. Vahala, "Soliton microcomb range measurement," *Science* **359**(6378), 884–887 (2018).

19. J. Riemsberger, A. Lukashchuk, M. Karpov, W. L. Weng, E. Lucas, J. Q. Liu, T. J. Kippenberg, "Massively parallel coherent laser ranging using a soliton microcomb," *Nature* **581**(7807), 164–170 (2020).

20. K. Y. Yang, J. Skarda, M. Cotrufo, A. Dutt, G. H. Ahn, M. Sawaby, D. Vercruyse, A. Arbabian, S. H. Fan, A. Alù, and J. Vučković, "Inverse-designed nonreciprocal pulse router for chip-based LiDAR," *Nat. Photonics* **14**, 369–374 (2020).

21. T. Tang, H.-J. Chen, Z. Y. Yuan, Y. Yu, Q.-T. Cao, N. An, Q. H. Gong, C. W. Wong, Y. J. Rao, Y.-F. Xiao, B. C. Yao, "Gain-assisted chiral soliton microcombs," *arXiv: 2008.12510* (2020).

22. Z. Shen, Y.-L. Zhang, Y. Chen, C.-L. Zou, Y.-F. Xiao, X.-B. Zou, F.-W. Sun, G.-C. Guo, and C.-H. Dong, "Experimental realization of optomechanically induced non-reciprocity," *Nature Photon.* **10**, 657 (2016).

23. Q.-T. Cao, H. Wang, C.-H. Dong, H. Jing, R.-S. Liu, X. Chen, L. Ge, Q. Gong, Y.-F. Xiao, "Experimental Demonstration of Spontaneous Chirality in a Nonlinear Microresonator," *Phys. Rev. Lett.* **118**, 033907 (2017).

24. Y. Shi, Z. Yu, and S. Fan, "Limitations of nonlinear optical isolators due to dynamic reciprocity," *Nat. Photonics* **9**, 388 (2015).

25. L. Fan, J. Wang, L. T. Varghese, H. Shen, B. Niu, Y. Xuan, A. M. Weiner, and M. Qi, "An All-Silicon Passive Optical Diode," *Science* **335**, 447 (2012).

26. S. Zhang, Y. Hu, G. Lin, Y. Niu, K. Xia, J. Gong, and S. Gong, "Thermal-motion-induced non-reciprocal quantum optical system," *Nat. Photonics* **12**, 744 (2018).

27. K. Y. Xia, F. Nori, and M. Xiao, "Cavity-Free Optical Isolators and Circulators Using a Chiral Cross-Kerr Nonlinearity," *Phys. Rev. Lett.* **121**, 203602 (2018).

28. M. Scheucher, A. Hilico, E. Will, J. Volz, A. Rauschenbeutel, "Quantum optical circulator controlled by a single chirally coupled atom," *Science* **354**, 1577 (2016).

29. A. Metelmann and A. A. Clerk, "Nonreciprocal Photon Transmission and Amplification via Reservoir Engineering," *Phys. Rev. X* **5**, 021025 (2015).

30. D. Malz, L. D. Tóth, N. R. Bernier, A. K. Feofanov, T. J. Kippenberg, and A. Nunnenkamp, "Quantum-Limited Directional Amplifiers with Optomechanics," *Phys. Rev. Lett.* **120**, 023601 (2018).

31. Z. Shen, Y.-L. Zhang, Y. Chen, F.-W. Sun, X. B. Zou, G. C. Guo, C.-L. Zou, and C. H. Dong, "Reconfigurable optomechanical circulator and directional amplifier," *Nat. Commun.* **9**, 1797 (2018).

32. X.-W. Xu, Y.-J. Zhao, H. Wang, H. Jing, and A.-X. Chen, "Nonreciprocal photon blockade via quadratic optomechanical coupling," *Photonics Research* **8**(2), 143–150 (2020).

33. X.-W. Xu, Y. Li, B. J. Li, H. Jing, and A.-X. Chen, "Nonreciprocity via Nonlinearity and Synthetic Magnetism," *Phys. Rev. Appl.* **13**(4), 044070 (2020).

34. D. L. Sounas and A. Alù, "Non-reciprocal photonics based on time modulation," *Nat. Photonics* **11**, 774 (2017).

35. N. Bender, S. Factor, J. D. Bodyfelt, H. Ramezani, D. N. Christodoulides, F. M. Ellis, and T. Kottos, "Observation of asymmetric transport in structures with active nonlinearities," *Phys. Rev. Lett.* **110**, 234101 (2013).

36. B. Peng, S. K. Özdemir, F. Lei, F. Monifi, M. Gianfreda, G. L. Long, S. Fan, F. Nori, C. M. Bender, and L. Yang, "Parity-time-symmetric whispering-gallery microcavities," *Nat. Phys.* **10**, 394 (2014).

37. L. Chang, X. Jiang, S. Hua, C. Yang, J. Wen, L. Jiang, G. Li, G. Wang, and M. Xiao, "Parity-time symmetry and variable optical isolation in active-passive-coupled microresonators," *Nat. Photonics* **8**, 524 (2014).

38. S. Maayani, R. Dahan, Y. Kligerman, E. Moses, A. U. Hassan, H. Jing, F. Nori, D. N. Christodoulides, and T. Carmon, "Flying couplers above spinning resonators generate irreversible refraction," *Nature (London)* **558**, 569 (2018).

39. H. Lü, Y. Jiang, Y. Z. Wang, and H. Jing, "Optomechanically induced transparency in a spinning resonator," *Photon. Res.* **5**, 367–371 (2017).

40. R. Huang, A. Miranowicz, J.-Q. Liao, F. Nori, H. Jing, "Nonreciprocal Photon Blockade," *Phys. Rev. Lett.* **121**, 153601 (2018).

41. B. J. Li, R. Huang, X.-W. Xu, A. Miranowicz, and H. Jing, "Nonreciprocal unconventional photon blockade in a spinning optomechanical system," *Photonics Research* **7**(6), 630–641 (2019).

42. R. Fleury, D. L. Sounas, C. F. Sieck, M. R. Haberman, and A. Alù, "Sound isolation and giant linear nonreciprocity in a compact acoustic circulator," *Science* **343**, 516 (2014).

43. Y. Jiang, S. Maayani, T. Carmon, F. Nori, and H. Jing, "Nonreciprocal phonon laser," *Phys. Rev. Appl.* **10**, 064037 (2018).

44. Y.-F. Jiao, S.-D. Zhang, Y.-L. Zhang, A. Miranowicz, L.-M. Kuang, and H. Jing, "Nonreciprocal Optomechanical Entanglement against Backscattering Losses," *Phys. Rev. Lett.* **125**, 143605 (2020).

45. H. Jing, H. Lü, S. K. Özdemir, T. Carmon, and F. Nori, "Nanoparticle

sensing with a spinning resonator," *Optica* **5**, 1424–1430 (2018).

- 46. J. Ahn, Z. Xu, J. Bang, P. Ju, X. Gao, and T. Li, "Ultrasensitive torque detection with an optically levitated nanorotor," *Nat. Nanotechnol.* **15**, 89 (2020).
- 47. H. L. Zhang, R. Huang, S.-D. Zhang, Y. Li, C.-W. Qiu, F. Nori, and H. Jing, "Anti-PT-symmetry-broken nonreciprocity in a linear resonator," *Nano Lett.* **20**, 7594–7599 (2020).
- 48. A. F. Runge, D. D. Hudson, K. K. Tam, C. M. De Sterke, A. Blancore-dondo, "The pure-quartic soliton laser," *Nat. Photonics* 1–6 (2020).
- 49. B. Corcoran, M. Tan, X. Xu, A. Boes, J. Y. Wu, T. G. Nguyen, S. T. Chu, B. E. Little, R. Morandotti, A. Mitchell, and D. J. Moss, "Ultra-dense optical data transmission over standard fibre with a single chip source," *Nat Commun* **11**, 2568 (2020).
- 50. A. Parriaux, K. Hammani, and G. Millot, "Electro-optic frequency combs," *Advances in Optics and Photonics* **12**(1), 223–287 (2020).
- 51. S. A. Diddams, K. Vahala, T. Udem, "Optical frequency combs: Coherently uniting the electromagnetic spectrum," *Science* **369**(6501), 267 (2020).
- 52. S. M. Spillane, T. J. Kippenberg, O. J. Painter, and K. J. Vahala, "Ideality in a Fiber-Taper-Coupled Microresonator System for Application to Cavity Quantum Electrodynamics," *Phys. Rev. Lett.* **91**, 043902 (2003).
- 53. G. B. Malykin, "The Sagnac effect: correct and incorrect explanations," *Phys. Usp.* **43**, 1229 (2000).
- 54. T. Qin, J. F. Yang, F. X. Zhang, Y. Chen, D. Y. Shen, L. Chen, X. S. Jiang, X. F. Chen, W. J. Wan, "Fast-and slow-light-enhanced light drag in a moving microcavity," *Communications Physics* **3**, 118 (2020).
- 55. L. A. Lugiato, R. Lefever, "Spatial dissipative structures in passive optical systems," *Phys. Rev. Lett.* **21**, 2209–2211 (1987).
- 56. Y. K. Chembo, and C. R. Menyuk, "Spatiotemporal Lugiato-Lefever formalism for Kerr-comb generation in whispering-gallery-mode resonators," *Phys. Rev. Lett.* **87**, 053852 (2013).
- 57. X. Yi, Q.-F. Yang, X. Zhang, K. Y. Yang, X. Li, and K. J. Vahala, "Single-mode dispersive waves and soliton microcomb dynamics," *Nat. Commun.* **8**, 14869 (2017).
- 58. S. Fujii, A. Hori, T. Kato, R. Suzuki, Y. Okabe, W. Yoshiki, T. Tanabe, "Effect on Kerr comb generation in a clockwise and counter-clockwise mode coupled microcavity", *Optics Express* **25**(23), 28969–28982 (2017).
- 59. D. Weiss, V. Sandoghdar, J. Hare, V. Lefevre-Seguin, J.-M. Raymond, and S. Haroche, "Splitting of high-Q Mie modes induced by light backscattering in silica microspheres," *Opt. Lett.* **20**, 1835–1837 (1995).
- 60. T. J. Kippenberg, S. Spillane, and K. Vahala, "Modal coupling in traveling-wave resonators," *Opt. Lett.* **27**, 1669–1671 (2002).
- 61. M. L. Gorodetsky, A. D. Pryamikov, and V. S. Ilchenko, "Rayleigh scattering in high-Q microspheres," *J. Opt. Soc. Am. B* **17**, 1051–1057 (2000).
- 62. W. Yoshiki, A. Chen-Jinnai, T. Tetsumoto, and T. Tanabe, "Observation of energy oscillation between strongly-coupled counter-propagating ultra-high Q whispering gallery modes," *Opt. Express* **23**, 30851–30860 (2015).
- 63. M. Aspelmeyer, T. J. Kippenberg, and F. Marquardt, "Cavity optomechanics," *Rev. Mod. Phys.* **86**(4), 1391 (2014).
- 64. C. Godey, I. V. Balakireva, A. Coillet, Y. K. Chembo, "Stability analysis of the spatiotemporal Lugiato-Lefever model for Kerr optical frequency combs in the anomalous and normal dispersion regimes," *Physical Review A* **89**(6), 063814 (2014).
- 65. E. Obrzud, S. Lecomte, T. Herr, "Temporal solitons in microresonators driven by optical pulses," *Nat. Photon.* **11**, 600 (2017).
- 66. D. C. Cole, J. R. Stone, M. Erkintalo, K. Y. Yang, X. Yi, K. J. Vahala, and S. B. Papp, "Kerr-microresonator solitons from a chirped background," *Optica* **5**, 1304–1310 (2018).
- 67. M. Shalaev, W. Walasik, A. Tsukernik, Y. Xu, and N. M. Litchinitser, "Robust topologically protected transport in photonic crystals at telecommunication wavelengths," *Nature Nano* **14**, 31–34 (2019).
- 68. S.-Y. Yu, C. He, X.-C. Sun, H. F. Wang, J.-Q. Wang, Z.-D. Zhang, B.-Y. Xie, Y. Tian, M.-H. Lu, and Y.-F. Chen, "Critical couplings in topological-insulator waveguide-resonator systems observed in elastic waves," *arXiv:2008.09547* (2020).
- 69. Z. W. Fan, and D. V. Skryabin, "Soliton blockade in bidirectional microresonators," *Opt. Lett.* **45**, 6446–6449 (2020)

## Supplementary Material: Nonreciprocal optical solitons in a spinning resonator

Baijun Li<sup>1</sup>, Sahin. K. Özdemir<sup>2</sup>, Lin Zhang<sup>3</sup>, and Hui Jing<sup>1,\*</sup>

<sup>1</sup>Key Laboratory of Low-Dimensional Quantum Structures and Quantum Control of Ministry of Education, Department of Physics and Synergetic Innovation Center for Quantum Effects and Applications, Hunan Normal University, Changsha 410081, China

<sup>2</sup>Department of Engineering Science and Mechanics, and Materials Research Institute, Pennsylvania State University, University Park, State College, Pennsylvania 16802, USA

<sup>3</sup>School of Physics and Information Technology, Shaanxi Normal University, Xi'an 710061, China

\*Corresponding author. Email: jinghui73@foxmail.com

## S1. EXPERIMENTAL FEASIBILITY OF THE SPINNING CAVITY

Our proposed scheme is experimentally feasible, the whispering-gallery mode resonator can be mounted on a turbine, which spins the resonator, as in the recent experiment [S1]. In the experiment, optical fiber can fly stably on the resonator with radius  $r = 1.1$  mm and rotation frequency  $\Omega = 6.6$  kHz, and achieve 99.6% optical isolation. By positioning the resonator near a single-mode telecommunication fiber, the light can be coupled into or out of the resonator evanescently through the tapered region. For a spinning device, the rapid rotation will drag air into the middle of the cavity and fiber, forming a thin layer of air. Due to air layer, the taper can fly at a height above the cavity, which can be several nanometers. When there is external disturbance that causes the taper to rise above the stable equilibrium height, the taper will float back to its original position, which is called "self-adjustment" [S1].

To further illustrate the "self-adjustment" effect, we perform a force analysis on the local deformation originated from air pressure of the tapered fiber. By cutting the fiber into a series of infinitesimal cylinders and focusing on the outermost one. The air pressure acting on the cylinder can be considered as  $\Delta T_{air} = (\rho \Delta \theta) T_{air} / L$  which leads to a tiny displacement  $d$ , where  $\rho(\theta)$  indicates the radius (angle) of the winding shape of the deformed region of the fiber. Then, the whole air pressure on the fiber can be calculated by [S1]

$$T_{air} = 6.19 \mu R^{5/2} \Omega \int_0^r (h - \sqrt{r^2 - x^2} + r)^{-3/2} dx, \quad (\text{S1})$$

where  $\mu$  is the viscosity of air,  $r(R)$  is the radius of the taper (resonator), and  $h = h_0 + d$  represents the taper-resonator separation, with the stationary gap between the fiber and the stationary sphere,  $h_0$ . Since the local deformation of the fiber, the tension on this infinitesimal cylinder can be estimated as

$$\Delta T_{en} = 2F \sin(\Delta\theta/2) \approx F\Delta\theta, \quad (\text{S2})$$

where  $F$  represents the elastic force on the taper and obeys the Hooke law,  $\sigma = eE$ . The  $\sigma = F/(\pi r^2)$  is the uniaxial stress,  $E$  is the Young modulus of silica, and  $e = \delta_L/L$  is the strain with  $\delta_L = L' - L$  denotes the length variation between the original length  $L$  and the deformation region  $L'$ . In the case of stable equilibrium, i.e.,  $\Delta T_{air} = \Delta T_{en}$ , we can obtain

$$T_{air} = 2\pi r^2 E [\arcsin(\phi) - \phi] \approx \pi r^2 \phi^3 / 3 \quad (\text{S3})$$

where  $\phi = 4Ld/(L^2 + 4d^2)$ , and we have used the approximation for  $|\phi| \ll 1$ ,  $\arcsin(\phi) = \phi + \phi^3/6 + \dots$ . Therefore, the displacement  $d$  can be analytically estimated as

$$d = \frac{L}{2} (\tau - \sqrt{\tau^2 - 1}) / 2 \quad (\text{S4})$$

where  $\tau = [\pi r^2 E / (3T_{air})]^{1/3}$ . Then, the strain of the taper can be rewritten as  $e = \arcsin(\phi)/\phi - 1 \approx \phi^2/6$ . From this expression, we find that the strain (i.e., the elastic force) is positively associated with the taper-resonator separation:

$$\frac{\partial F}{\partial h} = \pi r^2 E \left( \frac{\partial e}{\partial d} \right) = \frac{16\pi r^2 E L^2 d (L^2 - 4d^2)}{3(L^2 + 4d^2)} > 0 \quad (\text{S5})$$

which clearly shows that when any perturbation causes the air gap gets larger than the stable-equilibrium distance, the elastic force becomes stronger. As a result, the taper can be dragged back to its equilibrium position, leading to the "self-adjustment" effect. The behavior enables separation the taper from the spinning resonator and critical coupling of light into the cavity, by which counter-circulating light experiences optical drag identical in size, but opposite in sign. More importantly, this experiment also shown that even if the taper is pushed toward the rotating resonator, the taper will not contact or stick to the resonator, which is the opposite of the static resonator (i.e., the taper may stick to the resonator through van der Waals forces and thus needs to be pulled back to break the connection).

## S2. FROM COUPLED MODE EQUATIONS TO LUGIATO-LEFEVER EQUATION (LLE)

The intracavity fields can be described by the mode coupling equations [S2, S3]

$$\frac{dA_l}{dt} = -[\frac{\kappa_{Al}}{2} + i(\omega_d - \Delta_F - \omega_0)]A_l + iJB_l - ig \sum_{l', l'', l'''} A_{l'} A_{l''} A_{l'''} + \frac{\kappa_l}{2} \delta l_0 f, \quad (\text{S6})$$

$$\frac{dB_l}{dt} = -[\frac{\kappa_{Bl}}{2} + i(\omega_d + \Delta_F - \omega_0)]B_l + iJA_l - ig \sum_{l', l'', l'''} B_{l'} B_{l''} B_{l'''}, \quad (\text{S7})$$

where  $A_l, B_l$  is intracavity field of mode  $l$  in the clockwise (CW) and counter-clockwise (CCW) modes, respectively and  $\delta$  is the Kronecker delta. Here, in order to ensure energy conservation, the sum only valid for condition  $\omega_{l'} + \omega_{l''} = \omega_{l'''} + \omega_l$ . The  $t$  is time, the  $\kappa_{Al, Bl} = \omega_l/Q$  is the dissipation rate and  $\omega_0$  is pump mode frequency.  $f = \sqrt{\kappa P / (\hbar \omega_d)}$  denotes the pump field intensity.

Now we switch the above equations in the frequency domain to those in the spatial or time domain [S4], i.e.,

$$A(\theta, t) = \sum_l A_l e^{i(\omega_l - \omega_0) - il\theta}, B(\theta, t) = \sum_l B_l e^{i(\omega_l - \omega_0) - il\theta}, \quad (\text{S8})$$

where  $A(\theta, t)$  and  $B(\theta, t)$  is the spatiotemporal slowly varying envelope of the total field of the CW and CCW modes, respectively, and  $\theta \in [-\pi, \pi]$  is the azimuthal angle coordinate in the cavity. Ignoring high-order dispersions ( $\xi_3, \xi_4, \dots$ ), i.e.,  $\omega_l = \omega_0 + \xi_1 l + \xi_2 l^2/2$ , we can obtain

$$\begin{aligned} \frac{\partial A(\theta, t)}{\partial t} &= \sum_l [\frac{A_l}{dt} + i(\xi_1 l + \frac{\xi_2}{2} l^2) A_l] \Gamma(\theta) \\ &= -[\frac{\kappa}{2} + i(\Delta_p - \Delta_F)] A(\theta, t) - i\xi_1 l A(\theta, t) \\ &\quad + iJB(\theta, t) - i\frac{\xi_2}{2} \frac{\partial^2 A(\theta, t)}{\partial \theta^2} + f \\ &\quad + \sum_l ig \sum_{l', l'', l'''} A_{l'} A_{l''} A_{l'''} \Gamma(\theta), \end{aligned} \quad (\text{S9})$$

$$\begin{aligned} \frac{\partial B(\theta, t)}{\partial t} &= \sum_l [\frac{B_l}{dt} - i(\xi_1 l + \frac{\xi_2}{2} l^2) B_l] \Gamma(\theta) \\ &= -[\frac{\kappa}{2} + i(\Delta_p + \Delta_F)] B(\theta, t) - i\xi_1 l B(\theta, t) \\ &\quad + iJA(\theta, t) - i\frac{\xi_2}{2} \frac{\partial^2 B(\theta, t)}{\partial \theta^2} \\ &\quad + \sum_l ig \sum_{l', l'', l'''} B_{l'} B_{l''} B_{l'''} \Gamma(\theta), \end{aligned} \quad (\text{S10})$$

where  $\Gamma(\theta) = e^{i(\omega_l - \omega_0)t - il\theta}$  and we have assumed that all modes have the same dissipation,  $\kappa_{Al, Bl} = \kappa = \omega_0/Q$ , and  $\Delta_p = \omega_d - \omega_0$ . The nonlinear coupling term can be transformed by two autocorrelations as [S5]

$$\sum_{l, l', l'', l'''} \sum_{l''''} A_{l'} A_{l''} A_{l'''}^* = \sum_l \sum_{l'', \eta} A_{l+\eta} A_{l''} A_{l''+\eta}^* \quad (\text{S11})$$

where  $\eta = l''' - l''$ . Under the transformation  $\theta \rightarrow \theta - \xi_1 t \bmod [2\pi]$  [S4],

we obtain the LLE of the coupled mode [S6]

$$\frac{\partial A(\theta, t)}{\partial t} = -[\frac{\kappa}{2} + i(\Delta_p - \Delta_F)]A(\theta, t) - i\frac{\xi_2}{2}\frac{\partial^2 A(\theta, t)}{\partial \theta^2} + iJB(\theta, t) + ig|A|^2A + f, \quad (\text{S12})$$

$$\frac{\partial B(\theta, t)}{\partial t} = -[\frac{\kappa_B}{2} + i(\Delta_p + \Delta_F)]B(\theta, t) - i\frac{\xi_2}{2}\frac{\partial^2 B(\theta, t)}{\partial \theta^2} + iJA(\theta, t) + ig|B|^2B. \quad (\text{S13})$$

Finally, using the transformations

$$\psi(\theta, t) = \sqrt{\frac{2g}{\kappa}}A^*(\theta, t), \quad \phi(\theta, t) = \sqrt{\frac{2g}{\kappa}}B^*(\theta, t), \quad \tau = \frac{\kappa}{2}t, \quad (\text{S14})$$

$$\Delta_p = -\frac{2\delta}{\kappa}, \quad \beta = -\frac{2\xi_2}{\kappa}, \quad \Delta_{\text{sag}} = \frac{2\Delta_F}{\kappa}, \quad F = \sqrt{\frac{2g}{\kappa}}f^*, \quad (\text{S15})$$

we can also obtain the normalized LLE, i.e.,

$$\frac{\partial \psi}{\partial \tau} = -[1 + i(\Delta_p - \Delta_{\text{sag}})]\psi + i|\psi|^2\psi - i\frac{\beta}{2}\frac{\partial^2 \psi}{\partial \theta^2} + iJ\phi + F, \quad (\text{S16})$$

$$\frac{\partial \phi}{\partial \tau} = -[1 + i(\Delta_p + \Delta_{\text{sag}})]\phi + i|\phi|^2\phi - i\frac{\beta}{2}\frac{\partial^2 \phi}{\partial \theta^2} + iJ\psi. \quad (\text{S17})$$

## REFERENCES

- [S1] S. Maayani, R. Dahan, Y. Kligerman, E. Moses, A. U. Hassan, H. Jing, F. Nori, D. N. Christodoulides, and T. Carmon, "Flying couplers above spinning resonators generate irreversible refraction," *Nature (London)* **558**, 569 (2018).
- [S2] X. Yi, Q.-F. Yang, X. Zhang, K. Y. Yang, X. Li, and K. J. Vahala, "Single-mode dispersive waves and soliton microcomb dynamics," *Nat. Commun.* **8**, 14869 (2017).
- [S3] Y. Liu, Y. Xuan, X. X. Xue, P.-H. Wang, S. Chen, A. J. Metcalf, J. Wang, D. E. Leaird, M. Qi, and A. M. Weiner, "Investigation of mode coupling in normal-dispersion silicon nitride microresonators for Kerr frequency comb generation," *Optica* **1**, 137–144 (2014).
- [S4] Y. K. Chembo, and C. R. Menyuk, "Spatiotemporal Lugiatto-Lefever formalism for Kerr-comb generation in whispering-gallery-mode resonators," *Phys. Rev. Lett.* **87**, 053852 (2013).
- [S5] Hansson T, Modotto D, and Wabnitz S 2014 *Optics Communications* **312**(0) 134–136
- [S6] Fujii S, Hori A, Kato T, Suzuki R, Okabe Y, Yoshiki W, Tanabe T 2017 *Optics Express* **25**(23) 28969–28982